Journal of Civil Engineering and Management
ISSN 1392-3730 / eISSN 1822-3605
2022 Volume 28 Issue 7: 509–522
https://doi.org/10.3846/jcem.2022.16957

STRUCTURAL RESPONSE AND DAMAGE EVALUATION OF A TYPICAL HIGHRISE RC BUILDING IN DUBAI UNDER AN EARTHQUAKE WITH SINGLE AND MULTIPLE PEAKS

Sayed MAHMOUD[1], Muhammad SALEEM[2*], Amal HASANAIN[3], H. EL-SOKKARY[1], Mohamed ELSHARAWY[1], Magdy GENIDY[3], Ayman ABD-ELHAMED[3, 4]

[1]*Department of Civil and Construction Engineering, College of Engineering, Imam Abdulrahman Bin Faisal University, P.O. Box 1982 – Dammam 31441, Kingdom of Saudi Arabia*
[2]*Department of Mechanical and Energy Engineering, College of Engineering, Imam Abdulrahman Bin Faisal University, P.O. Box 1982 – Dammam 31441, Kingdom of Saudi Arabia*
[3]*Faculty of Engineering at Mataria, Helwan University, Cairo, Egypt*
[4]*Faculty of Engineering, King Salman International University, South Sinai, El-Tur, Egypt*

Received 4 December 2021; accepted 14 April 2022

Abstract. Seismic design codes predominantly assume that earthquakes involve a single ground shaking event; however, earthquakes can occur as a series of shocks. Consequently, the capacity of structures to resist earthquakes with multiple peaks without suffering severe damage is a crucial parameter. This research study evaluates the seismic performance of a high-rise building in Dubai using existing records of single and multiple peaks. Three-dimensional building model was developed considering the actual cross-sections of the horizontal and vertical elements fitting the seismic zone through dynamic response spectrum analysis. The building is analyzed using the nonlinear regime employing fast-nonlinear time-history analysis with the scaled NS and EW records of the Niigata earthquake. The main finding of this work is that records with multiple peaks significantly increase structural response and magnify the structural damage compared with records of single-peak earthquakes; thus, earthquakes involving multiple shocks significantly increase the risk of structural failure in a building.

Keywords: high-rise building, earthquake with single and multiple peaks, dynamic response, damage assessment.

Introduction

Typically, people in Gulf countries believe that they are not within an active seismic zone and that they need not be overly concerned about the occurrence of severe ground shakings; however, the risk of earthquakes is, in fact, a reality. Given the proximity of Iran to the United Arab Emirates (UAE), when severe ground motion occurs in the former, the northern part of the latter, specifically Dubai, which has numerous high-rise buildings, experiences moderate ground shakings. When an earthquake with a magnitude of 5.1 on the Richter scale hit the southern part of Iran, light ground shakings were reported across Dubai and the northern part of the UAE. Further, in April 2013, a powerful earthquake of magnitude 7.8 hit the border between Iran and Pakistan, resulting in one of the largest ground-motion events ever experienced in Dubai; this event led to the evacuation of thousands of people from high-rise buildings, with the subsequent revision of seismic design codes wherein the magnitude of the reference earthquake was increased from 5.0 to 5.9.

The earthquake-resistant design of structures requires the resulting inelastic responses to be within the acceptable limits provided by the seismic design codes. These adequate levels are commonly provided under the scenario of a single earthquake load. Similarly, the seismic design methods outlined in the recent seismic design codes related to the design of concrete structures are primarily based on single earthquakes whereas the effects of multiple earthquakes or "seismic sequences" within a short duration are barely considered (Abdelnaby, 2012; Di Sarno, 2013; Chandramohan et al., 2016). The induced seismic response, including the shear and flexural demands on the structural elements, may be affected when subjected

*Corresponding author. E-mail: *mssharif@iau.edu.sa*

to sequential ground motions. Thus, an efficient procedure is needed that considers the effects of seismic sequences during the design stages in terms of the threat to service-life during potential future earthquakes.

Following the Tohoku earthquake, which involved several aftershocks and recorded a huge magnitude of 9 on the Richter scale, loss of stiffness and strength in various structural elements or even whole structures was reported throughout the affected regions in Japan, which ultimately resulted in significant damage (Pomonis et al., 2011). Further, the great Niigata Ken Chuetsu earthquake, which occurred on October 23, 2004, with a magnitude of 6.6 on the Richter scale, was one of the most significant ground-motion events to strike Japan, causing severe structural damage and the destruction of numerous buildings in Niigata, with several buildings having entirely collapsed (Scawthorn & Rathje, 2006). Another devastating sequential earthquake occurred in central Italy in August 2016 and caused substantial damage as well as loss of lives in both the city at the center of the earthquake and the surrounding regions (Zimmaro et al., 2018). Therefore, verifying the capacity of building structures to resist sequential ground-motion events without failure or even total collapse is a crucial concern for specialists in this field. However, the effect of multi-shock earthquakes on high-rise buildings has not received considerable attention. Elnashai et al. (1998) were the first to discuss the effect of multiple earthquakes on structures when they analyzed the characteristics of the input motions and output response together with the dynamic behavior of building structures. Numerous years later, several studies have focused on the response of elasto-plastic SDOF building models under mainshock-aftershock acceleration records for the purpose of seismic response evaluation or seismic design in terms of ductility demand, behavior factor, inelastic displacement, damage and input energy (Amadio et al., 2003; Luco et al., 2004; Saleem & Tsubaki, 2010; Saleem & Nasir, 2016; Hatzigeorgiou & Beskos, 2009; Hatzigeorgiou, 2010; Goda & Taylor, 2012; Yaghmaei-Sabegh & Ruiz-García, 2016; Zhai et al., 2016; Wen et al., 2018). Because multiple degree of freedom (MDOF) systems can efficiently simulate real structures under cyclic loadings, other researchers have focused on MDOF systems to explore the induced responses to sequential earthquakes. Faisal et al. (2018) investigated the effect of multiple-shock earthquakes on the induced peak responses of three-dimensional (3D) inelastic concrete frames modeled as MDOF systems. Elsewhere, Parisi and Augenti (2013) investigated the effect of the sequential earthquake that occurred in L'Aquila, Italy in 2009 on the monumental masonry constructions there, with the authors noting the recorded levels of damage. Similarly, Penna et al. (2014) examined the damage to historical masonry buildings located in the region affected by the 2012 Emilia sequential earthquake. Ruiz-García and Negrete-Manriquez (2011) performed an investigation to understand the seismic response of MDOF systems to artificial and as-recorded mainshock–aftershock sequences. Generated mainshock–aftershock sequences using three different approaches in terms of repeated, randomized and as-recorded seismic sequences have been applied to four-story moment-resisting frame modelled as MDOF system to investigate the effect of different damage states on structural collapse capacity (Li et al., 2014). Parekar and Datta (2020) studied the effect of stiffness irregularity on seismic response demands of steel moment-resisting frames of three different heights subjected to under mainshocks-aftershocks seismic sequences through comparing the induced results with the mean seismic response demands of regular frame systems. Further investigations have been carried out to study the effect of such earthquake with multiple peaks on the assessment of damage of box girder bridges modelled as SDOF system (Ghosh et al., 2015) and moment-resisting frame modelled as MDOF system (Jalayer & Ebrahimian, 2017).

The response of RC buildings of 3- and 5-story height under mainshock-aftershock seismic sequences has been examined considering regularity and irregularity in elevation of each building (Hatzivassiliou & Hatzigeorgiou, 2015). Ruiz-García et al. (2018) performed an investigation to gain further understanding of the response of 3-D framed steel buildings subjected to real mainshock-aftershock seismic sequences. The safety assessment and seismic response of a containment structure subjected to near- and far-fault seismic sequences have also been studied (Bao et al., 2019). Analyses to investigate the damage evolution under repeated seismic records of masonry structures modelled as a SDOF system under the Central Italy seismic sequence employing the Park & Ang index to quantify the damage evolution has been carried out (Goda & Salami, 2014). Goda and Salami (2014) investigated the effect of aftershocks on seismic fragility of conventional wooden frames in south-western British Columbia, Canada. The analyses of wooden structures to include the influence of seismic sequences of smaller-magnitude events on damage and seismic losses for light-frame wood buildings has been also conducted (Chase et al., 2019). Soureshjani and Massumi (2022) investigated the behavior of RC moment-resisting buildings with shear walls to seismic sequences employing explicit time-history analysis. The developed structural models of the buildings were of three and six stories.

Most of the previously cited research works studied moment-resisting frames, idealized as SDOF or MDOF systems, to get some insights into the effect of earthquakes with multiple peaks on the induced seismic response of buildings. The current research work presents a comprehensive study pertaining to multiple-earthquake hazards through investigating the seismic responses and damage assessment of a typical high-rise RC building in Dubai under an earthquake with single and multiple peaks. Real records with single and multiple peaks from Niigata earthquake are used to excite the building in two orthogonal directions separately. The induced structural responses are

investigated in terms of the seismic sequences effect and the seismic response demand due to design spectra. In addition, damage of the considered building to the selected records are also provided.

1. Structural models

The building considered herein (henceforth referred to as "building") is situated in Dubai, a major city in the UAE. Given its close proximity to Iran, Dubai is susceptible to earthquake-related ground shakings. The building's structure follows a geometrically irregular structural scheme, as shown in Figure 1. The plan of the high-rise building covers an area of around 2,100 m^2, presenting an almost rectangular shape characterized by abundant nets of shear walls (see Figure 2). The proposed building system is a skeleton-type system with rigid-cast in-situ reinforced concrete (RC) columns, slabs, beams, and shear walls. This presents an appropriate system owing to its flexibility, limited maintenance requirements, and relatively low cost. The ground floor is 6.15 m in height, the first- and typical-floors heights are 3.8 m and 3.5 m, respectively. The base of the building is located 3.65 m below the ground floor (z = 0 m), and the roof of the building is at level z = 86.30 m. The columns are mainly distributed within the perimeters of the basement and the ground floor, with the maximum height measured from a foundation level of around 6.15 m and rectangular cross sections. The beams are distributed as perimetrical and intermediate L- and T-sections, respectively. In addition, spandrel beams with varied widths of 300 to 400 mm and depths of 1,200 to 3,700 mm are used to connect the shear-wall wings. The foundation system comprises piles and cap piles under the vertical elements in terms of shear walls and columns used to adequately support the weight of the structure itself and any imposed loads through multiple soil layers.

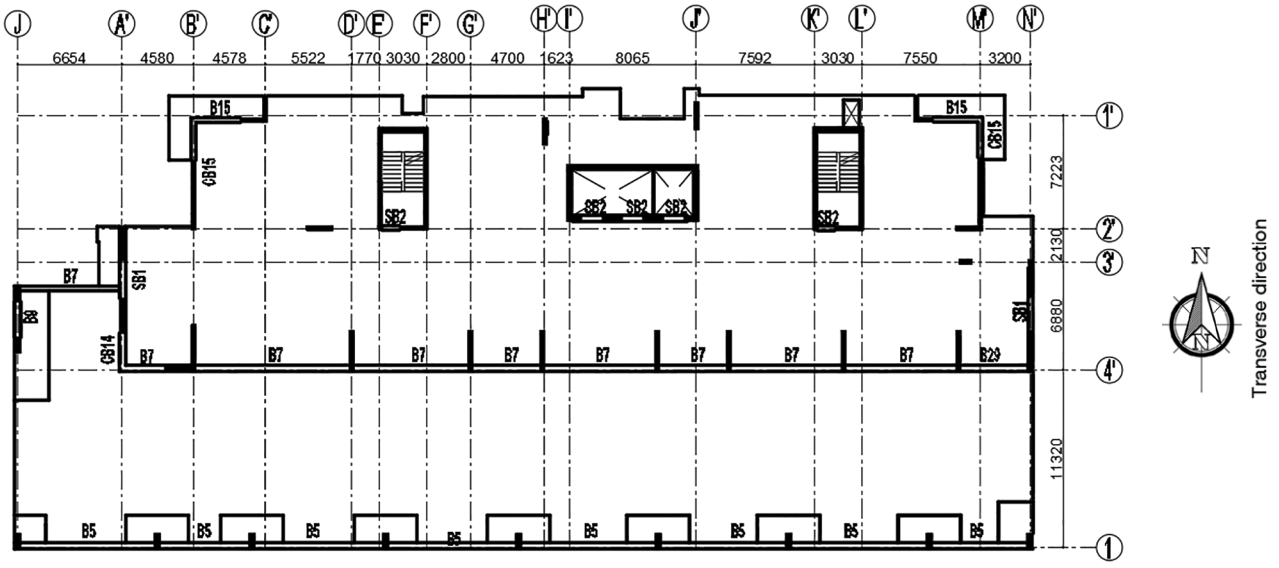

Figure 1. Plan view of the overall framing layout for the basement and ground floor

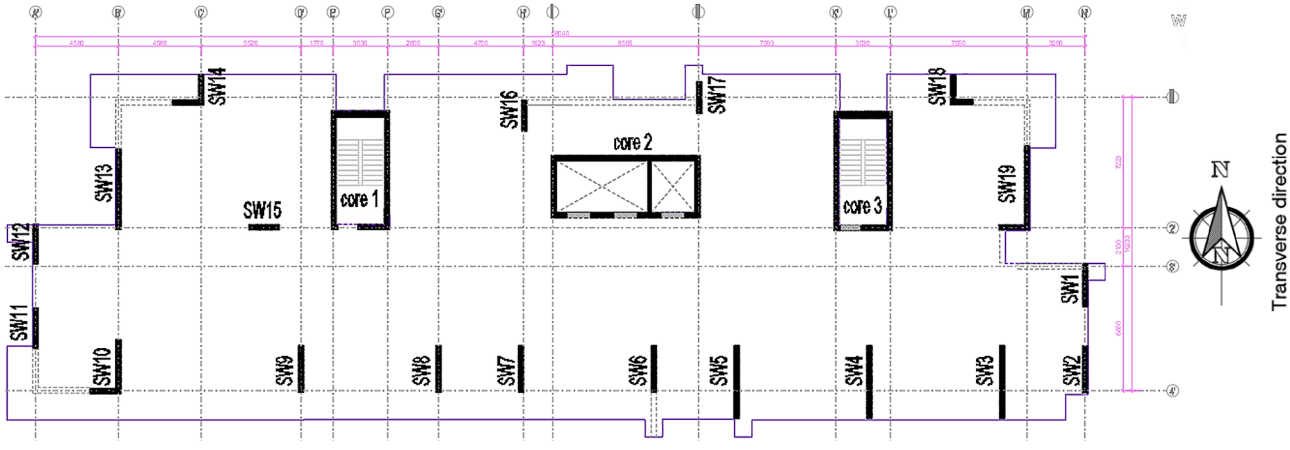

Figure 2. Plan view of the labeled-shear-wall layout for typical floors

1.1. Numerical model

A 3D model of the high-rise building was created using the ETABS software structural package as shown in Figure 3. The beams, girders, and columns were modeled as frame-type elements, with the beams and girders directly supported by the columns and, in places, by shear walls. The common practice in structural software package ETABS for modelling and analysis of RC beam-column connections is center to center modeling of horizontal and vertical elements as frame elements which implies that these members are connected together at their centers. During the elastic stage of analysis, the modelled frame elements follow Euler-Bernoulli beam theory. However, plastic hinges at both ends of frame elements are assigned for the plastic response stage. Geometrical and material nonlinearities are considered in order to properly simulate the behavior of connections. Slabs of varying thicknesses from 250 to 350 mm were modeled using shell-type finite elements. For the slabs directly supported by the columns and shear walls, drops or so-called "drop panels" with a total thickness ranging from 400 to 600 mm were required and were also modeled as shell-type elements. A semi-rigid diaphragm was assigned to the slabs during performing the analysis. The shell-like form was again utilized to model the shear walls, whereas fixed supports were used to model the foundations. For accurate simulation and prediction of the behavior of RC shear walls in terms of shear and flexure for nonlinear earthquake response analysis, the shear walls are modeled by using shell finite elements in the webs and in the boundary regions of walls as well. The modelling process includes rectangular meshes of predefined size employing the automatic rectangular mesh settings for walls. The assigned frame elements were divided into numerous sub-elements to distribute the structure's mass across various nodes. A typical building design was adopted for the structural elements, particularly the vertical elements, using 3D modeling incorporating the American Society of Civil Engineers' [ASCE] (ASCE 7-16) load combinations for the gravitational and seismic loads (ASCE, 2017). The seismic mass was lumped at the center of mass of each floor. The seismic analysis involved a modal spectral analysis incorporating the design spectra associated with the seismic intensity used for the design of structural elements in Dubai. The equivalent static force (ESF) procedure was adopted to calibrate the dynamic base shear with the static shear as per the seismic design code. The lateral (story) drifts and deformations were extracted from the developed 3D model to represent the degree of cracking under the maximum seismic load, which ensured the maximum seismic drift at the top of the building did not exceed the permitted value stated in the design code approved by the authorities. The stiffness modifiers used to perform the dynamic analysis of the created model were 0.35 and o.25 of the gross section moment of inertia (I_g) of the beams and the conventional RC slabs, respectively. For the cracked and uncracked walls, we used stiffness modifiers with values of 0.35 and 0.7 I_g, respectively while the I_g of the columns was reduced by 0.7. The models were created using a concrete density of $\gamma_c = 24$ kN/m^3, with a compressive strength of $f_c^{'} = 55$ MPa for the columns and walls and $f_c^{'} = 40$ MPa for the slabs, beams, and stairs. The reinforcing steel used in the developed model was deformed high-strength high-bond steel, with minimum yield strengths of 460 and 420 N/mm^2 for flexural and shear reinforcements, respectively.

2. Material properties

The properties of the concrete and reinforcing steel materials were specified according to the nominal values stated in the construction blueprints for performing the

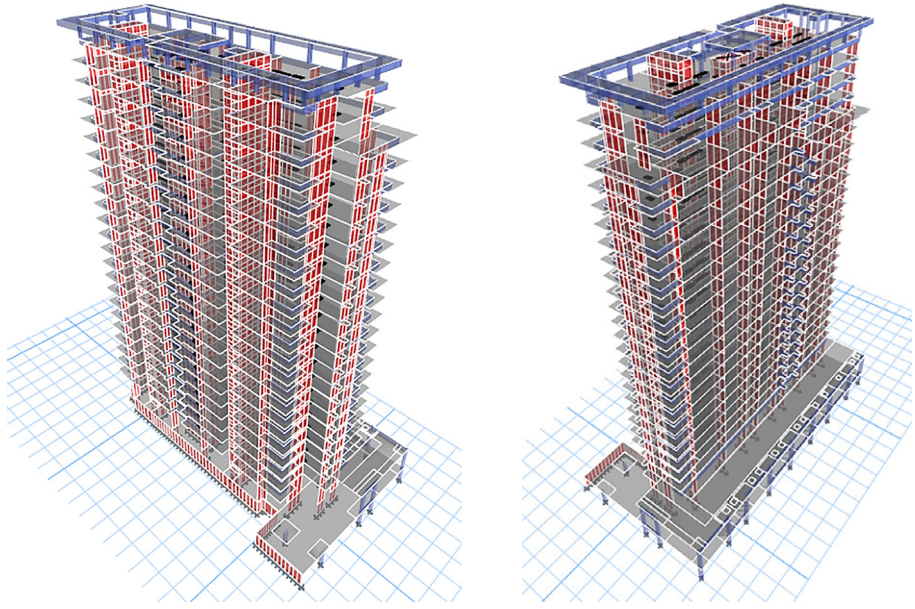

Figure 3. Three-dimensional (3D) model of the high-rise building

initial analysis of the structural model. In the blueprints, the characteristic compressive strength values of concrete were specified to be 55 and 40 MPa, respectively. The former of these values was adopted for the design and analysis of the supporting RC piles, shear walls, and columns, whereas the latter value was adopted for the horizontal elements such as the beams and slabs. The yield strength values of the steel reinforcing bars were set to 460 and 420 MPa for the main and transverse reinforcement, respectively. For the current study, the modulus elasticity of concrete was calculated in terms of the assigned compressive strength value as $4700\sqrt{f_c'}$. The modulus of elasticity of the steel reinforcement bars used in the analysis was 200,000 MPa. The chosen structural software package is capable of handling any material model in addition to those adopted in the current work, i.e., the concrete and reinforcing steel material model shown in Figure 4. Figure 4 presents the developed stress–strain relationship of concrete in compression and tension as developed by the computer program. For simulating compression, the stress–strain relationship was modeled using a parabolic curve that reached the maximum specified strength before a decreasing linear response occurred until the crushing strain limit was reached, indicating failure. The typical stress–strain relationship of the reinforcing steel under tension and compression is also presented in Figure 4. As can be clearly observed therein, the induced behavior of the steel bars was almost linearly elastic up to the yielding point. With a further increase in stress, a corresponding strain was observed in the steel, forming a strain-hardening region up to ultimate strength point.

3. Seismic demand

Many cities worldwide are prone to major earthquakes. The UAE is located on the margins of the Arabian Tectonic Plate, which can move toward the north to collide with the Eurasian Plate. Such a collision pushes up the tectonic plate constituting the Zagros Mountains of Iran, which is considered to be one of the most seismically active regions in the world, thus endangering numerous sites. Dubai city, known for its incredible skyline of towering skyscrapers, can be regarded as among them, given the UAE's close proximity to Iran. The city's municipality ruled that any newly built tower of over ten floors should have the capacity to withstand a 5.9-magnitude earthquake. The seismic design codes adopted by the authorities in Dubai provide a seismic zone intensity of 0.2 g (Mwafy et al., 2006). Thus, seismic events are a concern for the city and sufficient research attention must be given to explicitly evaluating how high-rise buildings are likely to perform during such unexpected excitations.

3.1. Earthquake data

The ground motions were selected from the data recorded for the Niigata region in Japan by Pacific Earthquake Engineering Research Centre (PEER) database. They were recorded on stiff soil within a distance varying between 9.79 and 23.05 km from the rupture fault. The event magnitudes (M_w) ranged from 6.6 to 6.8 on the Richter scale. The selection of the earthquake records is one of the most important factors in dynamic time–history analysis wherein the induced responses mainly depend on the characteristics of the selected ground-motion records. The selection criteria for the records included the existence of pulses in which multiple peaks occurred closely in terms of both time and location, which were crucial to our focus on the effect these multiple peaks have on the design capacity. The appropriate indicator for determining the frequency content of the ground motion was deemed to be the ratio of PGA to PGV. The selected records were of approximately moderate-frequency content while the time duration varied from 260 to 300 s. Dynamic fast nonlinear analyses were conducted using the ETABS program, which was specifically developed for the structural analysis and design of buildings by CSI. The analyses were performed using the NS and EW components as the input along the transverse and longitudinal directions of the 3D model, respectively. The earthquake excitation records used in the analysis are presented in Figure 5.

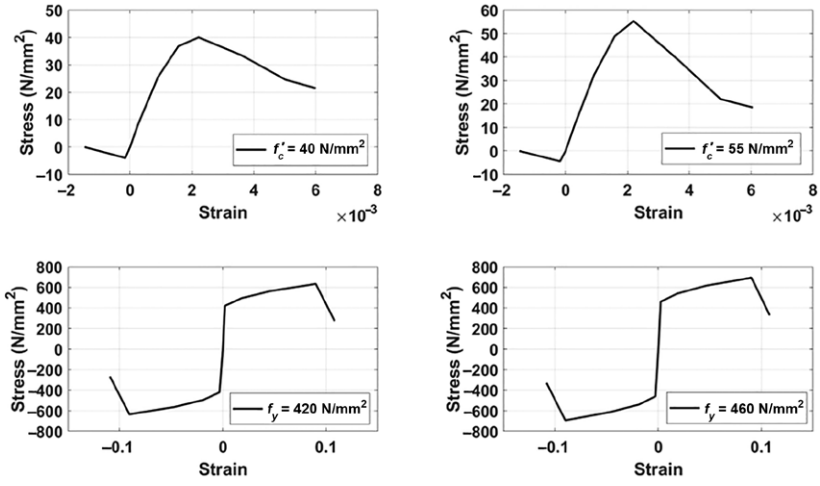

Figure 4. Stress–strain relationship of concrete and reinforcing steel under tension and compression

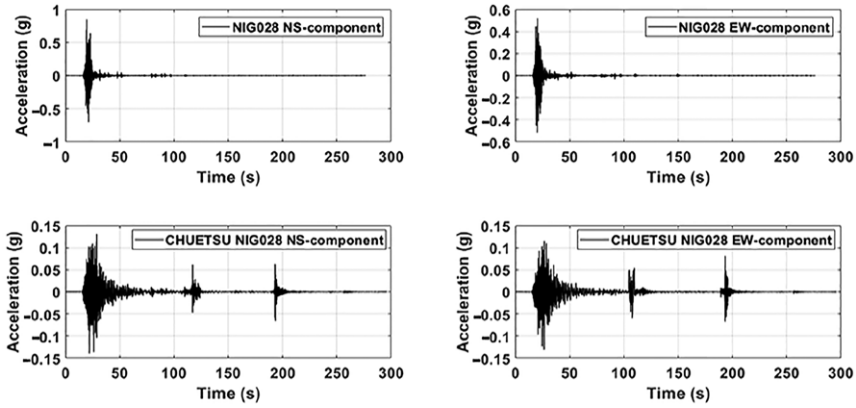

Figure 5. Ground motions inputted into the developed building model

3.2. Response spectrum analysis

The response spectrum (RS) analysis procedure based on ASCE 7-16 (ASCE, 2017) was adopted herein for seismic-demand design purposes. Based on the RS, the computed elastic response from the modes of interest were combined to obtain the overall response using the square root of the sum of the squares (SRSS), a method recommended in the code. To obtain the design force values, the response reduction factor (R) was used to reduce the obtained total elastic response. The modes of interest in the direction of loading should have achieved around 90% or more of the participating mass ratio. In accordance with the ASCE 7-16 standard (ASCE, 2017), the calculated design base shear using the RS procedure should have fulfilled at least 85% of the calculated base shear from the equivalent static analysis procedure. Further, a deflection amplification factor (C_d) was used to adjust the floor displacement and drift results calculated from the RS analysis. The scaling base shear factor and the importance factor were also used to scale up the computed story moments and the story shear forces as required by the ASCE 7-16 standard (ASCE, 2017). Owing to the building's irregularity and the consequent torsional sensitivity, the static analysis was only appropriate for the base calibration and not for the seismic design, as is recommended by the seismic design code. The typical RS curve provided by the ASCE 7-16 standard (ASCE, 2017) can be defined in terms of two ordinate values, S_{DS} and S_{D1}, which are regarded as the design spectral response acceleration at short and at 1-s periods, respectively, as shown in Figure 6. These two parameters can be evaluated based on the velocity and acceleration site coefficients F_v and F_1 as well as the spectral acceleration values S_s and S_1, respectively:

$$S_{DS} = \frac{2}{3}\left(F_a.S_s\right); \tag{1}$$

$$S_{D1} = \frac{2}{3}\left(F_v.S_1\right). \tag{2}$$

4. Damage index calculation

To quantify the damage sustained by the structure under applied dynamic loads, various damage indices have been proposed and introduced in terms of structural deformation, structural ductility, dissipated energy, and stiffness degradation (Park & Ang, 1985; Hameed et al., 2012; Powell & Allahabadi, 1988; McCabe & Hall, 1989; Kunnath et al., 1990; Williams & Sexsmith, 1995). Measuring the damage of building structures subjected to earthquake loads is predominantly based on the parameters related to the dynamic response of the building model. Damage as a measurement indicator, the damage indices were based on the results of the dynamic analysis. In addition to the induced deformation to the structure, which is a key parameter for identifying structural damage under dynamic

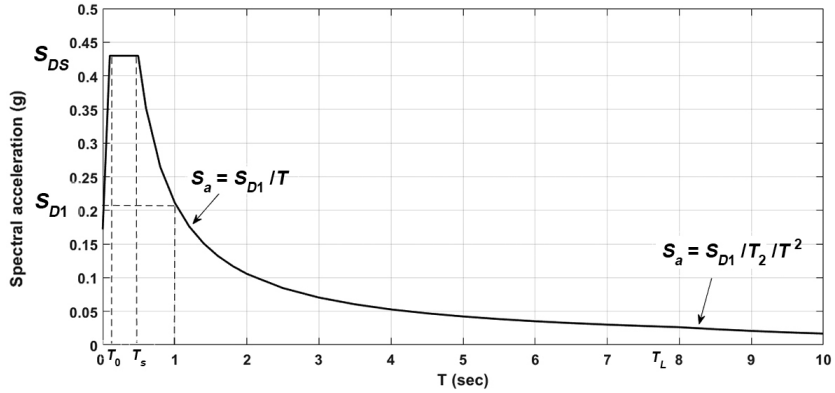

Figure 6. Response spectrum curve obtained for Dubai according to the ASCE 7-16 standard (ASCE, 2017)

loadings, the concept of plastic energy was used to determine the structural damage. The developed damage indices corresponding with the induced structural response could be classified in terms of building deformation as deformation-based models. Furthermore, energy-based damage indices correlated with the concepts of cyclic deterioration were adopted as another class of the developed models while a combination of the deformation- and energy-based damage indices models formed another class. One of the most commonly used damage indices is that introduced by both Fajfar (1992) and Cosenza et al. (1993), in which the damage of the structure is expressed in terms of the induced absorbed hysteretic energy (E_H), yield strength (f_y), yield displacement (U_y), and ultimate ductility (μ_u) as follows:

$$DI_{FC} = \frac{E_H / f_y U_y}{\mu_u - 1}. \quad (3)$$

The ultimate displacement and yield displacement achieved under the applied dynamic load are related through the ultimate ductility as $U_u = \mu U_y$. The structural damage index provided herein correlates with the damage caused by excessive displacement and the damage caused by the repeated cyclic loading effect. The commonly used values of damage indices for describing the state of the structure were categorized into specific ranges. Damage index values of < 0.25 signify slight or minor damage, values in the range of 0.25–0.40 signify moderate damage, and values in the range of 0.4–0.80 signify severe damage. Structural failure or collapse is expected to occur when the damage index value is >0.8.

5. Results and discussion

5.1. Case study

The seismic response of a high-rise building with a shear-wall system was investigated under the NS and NE components of the Niigata earthquake ground motions recorded as single and multi-shock earthquakes in the transverse and longitudinal directions of the building. Herein, the selected ground motions for the time–history analysis were scaled to 0.2 g to fit the seismic intensity of Dubai. RS analysis was performed using the developed model of the high-rise building for calculating the design response quantities of interest viz., floor acceleration, displacement, shear force, and the overturning moment. A value of $R = 4$ was used for performing the RS analysis, with a deflection amplification factor of $C_d = 4$. The design acceleration response spectrum values for Dubai with a velocity site coefficient $F_v = 2.2$ and an acceleration site coefficient $F_a = 1.4$ for stiff soil were calculated. A constant modal damping ratio of 5% was used to perform the dynamic RS analysis according to ASCE-7-16 requirements. The utilized effective moments of inertia for the RC vertical elements in terms of walls and columns and the horizontal elements in terms of RC beams and slabs were assigned according to the percentage values stated in the design code. The equivalent static method was employed to calibrate the induced design shear at the base under the RS method. The participating mass ratios for the assumed number of modes were found to be 99.03%, 99.24%, and 96.88% for the x-, y-, and z-directions, respectively. These captured values exceeded the 90% value recommended by the design code to represent the dynamic response of the building in the spectral analysis. The structural response of the high-rise building from the time–history and RS analyses were reported in terms of the peak floor acceleration, displacement, peak story shear force, and peak story overturning moment values.

5.2. Story acceleration response

Peak floor acceleration is an important factor that affects the responses of the installed nonstructural elements of the structure. Several studies on earthquake effects conducted over recent decades reveal that the number of injured persons, the number of fatalities, and the repair costs are mainly related to the failure of the nonstructural elements due to the induced acceleration responses that exceeded the limits associated with damage. Figure 7 shows the variation of the obtained peak acceleration responses at each floor level of the high-rise building of interest in the longitudinal and transverse directions. As can be clearly observed in Figure 7, the plotted curves indicate much larger peak floor acceleration responses under the Niigata seismic records with pulses compared with those obtained for the Niigata records *without* pulses, for both the NS and EW records. The difference resulting from the variation in earthquake type is more pronounced at the top story of the structure, regardless of the loading direction. Considering the 25th floor (top floor) of the building as an example, the peak floor acceleration values reached close to 0.72 g (without pulses) and 1.30 g (with pulses), which are almost three and a half and six times the scaled PGA of the corresponding Niigata records in the NS direction, respectively. Similarly, the peak floor acceleration reached close to 0.88 g (without pulses) and 1.49 g (with pulses), which are almost four and seven times the scaled PGA of the corresponding Niigata records in the EW direction, respectively. Figure 8 presents the induced story accelerations using the dynamic RS method in the transverse and longitudinal directions. The achieved peak floor acceleration values obtained when applying the dynamic RS analysis for design purposes are close to 0.77 and 0.86 g. These values are nearly four times the seismic intensity of the Dubai region. The obtained dynamic time–history results under single Niigata records indicate a very slight difference compared with the dynamic RS analysis results analyzed in the two directions. In contrast, the dynamic time–history analysis results obtained through the Niigata records with sequences significantly exceeded the induced peak acceleration design results obtained via the RS analysis method. Consequently, records that contain sequences can induce significant economic loss related to the damage to nonstructural elements and systems due to the magnification of the acceleration responses above the design values.

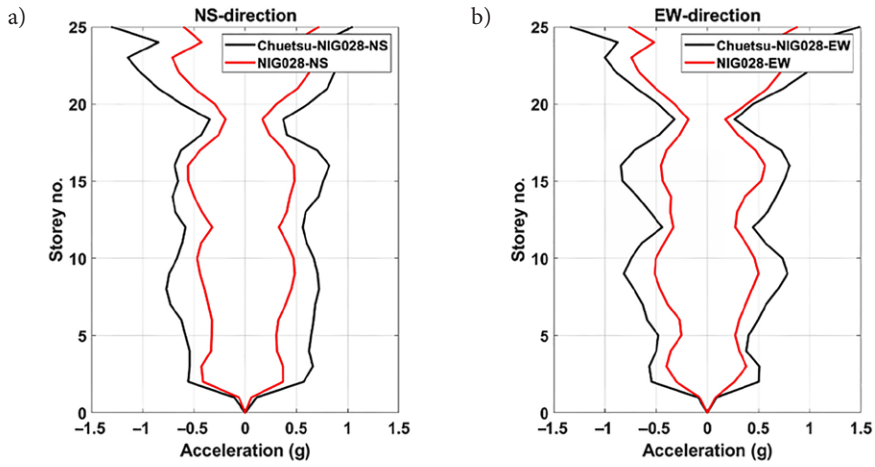

Figure 7. Peak story acceleration curves of the high-rise building vs. story number under the NS and EW components of the Niigata records with and without sequences in the: a – transverse direction and b – longitudinal direction

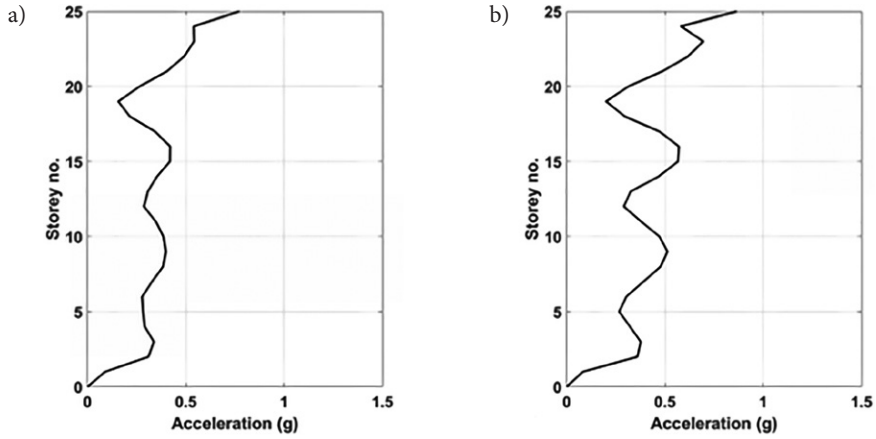

Figure 8. Peak story acceleration curves vs. story number under RS analysis in the: a – transverse direction and b – longitudinal direction

5.3. Story displacement response

The plotted curves of the obtained maximum displacement values at each story level for both the NS and EW components of the selected Niigata earthquake records scaled to 0.2 g are presented in Figure 9 in terms of both the longitudinal and transverse directions. Here, the peak displacement results at each story level are observed to be significantly influenced in both directions of analysis under the Niigata records with sequences. In particular, the attained peak displacement values with and without sequences reveal that the maximum values attained in the former were higher than those attained in the latter for both the longitudinal and transverse directions. The captured maximum displacement responses were significantly different under the Niigata records with and without sequences for the same direction of analysis and slightly different for the other direction of analysis. Under the NS components of the Niigata earthquake with and without sequences in the longitudinal direction, the induced maximum floor horizontal displacements were around 265 and 155 mm, respectively. The corresponding maximum floor horizontal displacements related to the EW components of the Niigata records with and without sequences were slightly higher at around 305 and 165 mm, respectively. Notably, the calculated percentage of increase in peak displacement responses under the records with sequences in the longitudinal direction were almost the same as that obtained under the records in the transverse direction.

Under the application of the RS load in the transverse and longitudinal directions, the induced maximum floor horizontal displacements were around 217 and 187 mm, respectively, as shown in Figure 10. These design values were higher than the dynamic time–history peak values obtained under the Niigata records without sequences and lower than those obtained under the Niigata records with sequences in both directions (see Figure 9 and Figure 10). In terms of the high-rise building of interest, the obtained maximum story displacement demand was observed to be at the top floor and depended on the existence of the sequences of the applied NS components of the ground motions. Similar observations were made for the EW records. Overall, the ground motion records with sequences generated the highest displacement demand compared with the induced displacement demand under both the dynamic RS and the Niigata records without sequences.

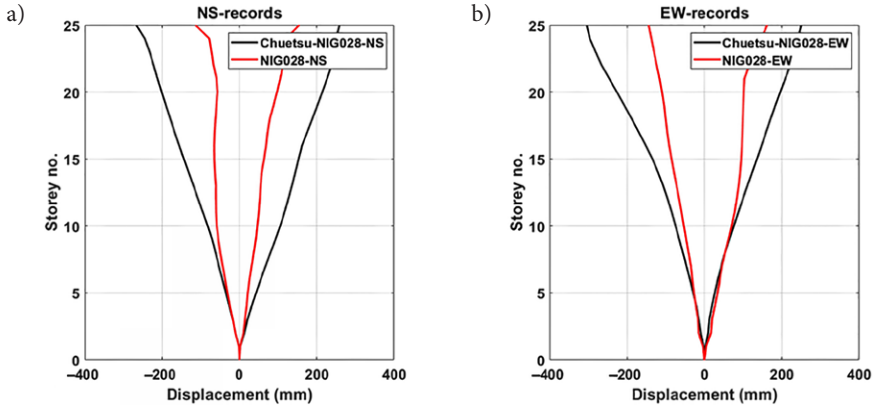

Figure 9. Peak story displacement curves vs. story number under the NS and EW components of the Niigata records with and without sequences in the: a – transverse direction and b – longitudinal direction

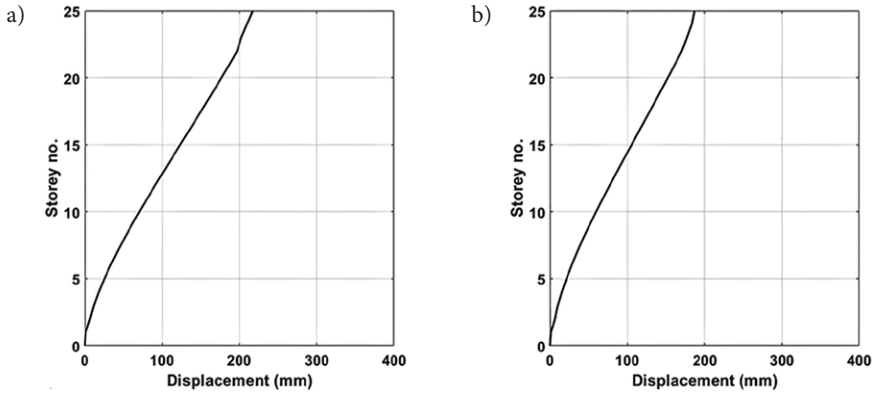

Figure 10. Peak story displacement curves vs. story number under RS analysis in the: a – transverse direction and b – longitudinal direction

5.4. Story shear response

Figure 11 illustrates the profiles of the induced peak story shear forces along the entire height of the high-rise building subjected to the Niigata records with and without sequences in both the transverse and longitudinal directions. The design story shear forces profiles obtained via the dynamic RS analysis according to the ASCE design code requirements are presented in Figure 12. As shown in Figure 11, for the transverse and longitudinal directions under the NS and EW records, the sequences incorporated in the Niigata records produced a significantly larger design shear envelope for the building than that produced under the Niigata records without sequences. A comparison of Figure 11 and Figure 12 clearly indicates that the estimated inelastic shear forces of the building under the Niigata records with sequences were not in accordance with the obtained design results when applying RS dynamic analysis in the transverse and longitudinal directions according to the ASCE seismic design code. However, the calculated peak story shear forces of the high-rise building subjected to the Niigata records without sequences greed well with the design shear forces obtained via the RS method. As a result of the existence of sequences in the excitation records, the calculated inelastic shear demands on the structural components of the building were significantly higher than those obtained both by applying the excitation records without sequences and the dynamic RS analysis, particularly in terms of the transverse direction. The captured peak shear force values at the base of the building using the spectrum design procedure were around 1.28×10^5 and 1.43×10^5 for the transverse and longitudinal directions, respectively. The ratio of the estimated design shear force demand to the shear demand obtained using the Niigata records with and without sequences in the transverse directions were found to be 51% and 11%, respectively. In terms of the longitudinal direction, the computed ratios were 31% and 9%, respectively. These observations suggest that, contrary to the common assumption, the spectrum design procedure may not represent ground-motion inputs with sequences when calculating the shear design of high-rise buildings. In contrast, the RS analysis produced shear results that slightly differed from those obtained under the Niigata records without sequences. These results indicate that earthquakes with multiple peaks play a significant role in magnifying the seismic force demand, particularly in the transverse direction.

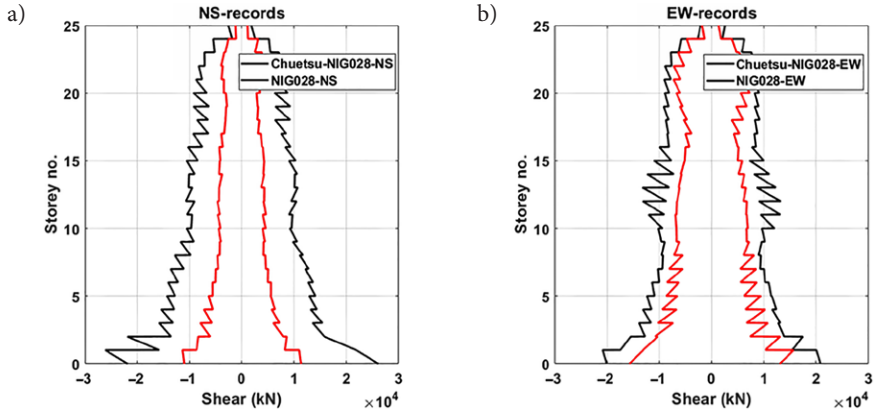

Figure 11. Peak story shear curves vs. story number under the NS and EW components of the Niigata records with and without sequences in the: a – transverse direction and b – longitudinal direction

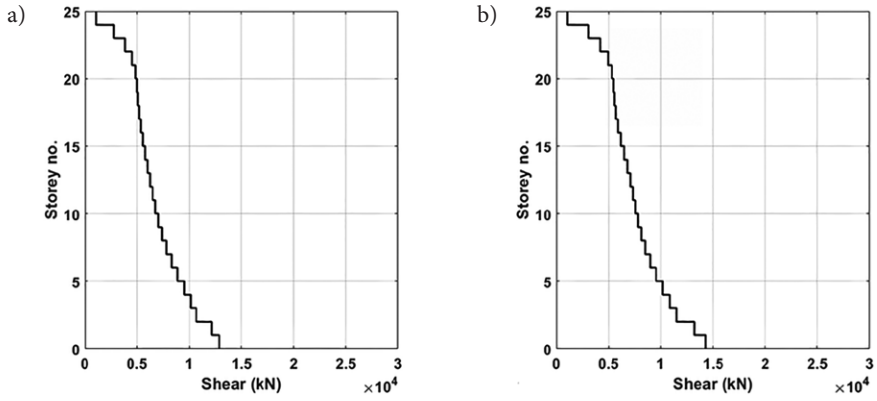

Figure 12. Peak story shear curves vs. story number under RS analysis in the: a – transverse direction and b – longitudinal direction

5.5. Story moment response

The peak moment results for each level of the high-rise building obtained via nonlinear time–history analysis using two types of ground motion are presented in Figure 13 in terms of both the transverse and longitudinal directions. A comparison of the plotted curves reveals that the peak story moment values resulting from the ground motions with sequences were higher than those resulting from ground motions without sequences in both the transverse and longitudinal responses. The moment demand on the building when subjected to earthquake motions with sequences tended to gradually increase in accordance with the story level, which caused an incremental build-up of base moment demand. Conversely, the lowest moment demand values were associated with the records without sequences along the timeline of the earthquake. In terms of the transverse direction, the induced peak story moment responses at the building's base were 9.81×10^5 and 5.69×10^5 kN.m under the NS records with and without sequences, respectively. The corresponding values in the longitudinal direction were 6.75×10^5 and 3.49×10^5 kN.m under the EW records with and without sequences, respectively. These values clearly indicate that the existence of sequences in the ground motion records considerably influenced the moment responses. Figure 13 shows that as the story level decreased, the discrepancy between the values of the induced maximum story moments significantly varied for the two types of ground motions, particularly in the transverse direction. As shown in Figure 13, the transverse direction attracted higher story moments than the longitudinal direction under the two types of records. This could be due to the arrangement of the shear walls runs mainly in the transverse direction, leading to an increase in stiffness in that direction compared with the longitudinal direction and a subsequent increase in straining actions in terms of story moments. The application of dynamic RS analysis for design purposes returned base peak story moment values of 4.26×10^5 and 5.74×10^5 kN.m in the transverse and longitudinal directions, respectively (see Figure 14). From a percentage perspective, these design values differed by around 18% and 4% from those obtained using the dynamic time–history analysis using the Niigata records without sequences. These ratios jumped to 37% and 40% when comparing the design results with the dynamic time–history analysis using the scaled Niigata records with sequences. These calculated ratios demonstrate a reasonable fit between the obtained dynamic RS results and dynamic time–history results of the scaled Niigata records without sequences. However, the story moments for the Niigata ground shakings associated with the presence of sequences exceeded the design RS values.

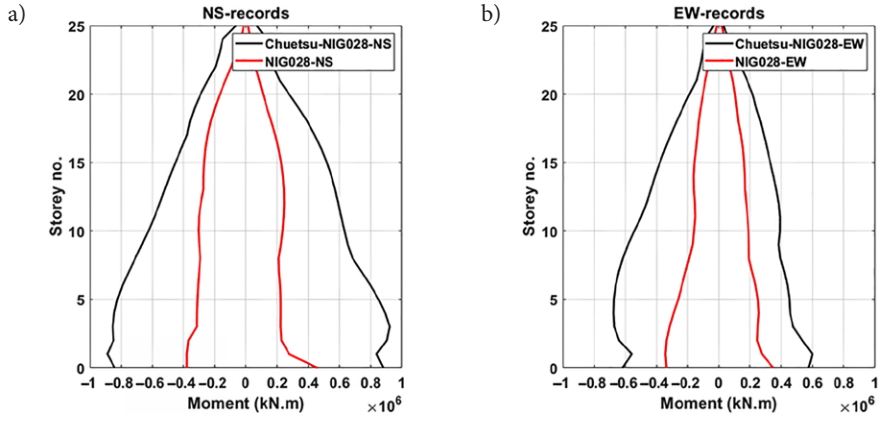

Figure 13. Peak story moment curves vs. story number under the NS and EW components of the Niigata records with and without sequences: a – transverse direction; b – longitudinal direction

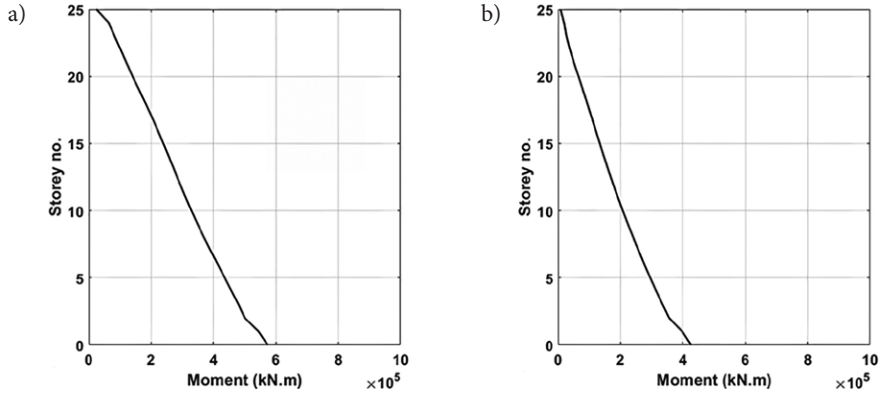

Figure 14. Peak story moment curves vs. story number under RS analysis in the: a – transverse direction and b – longitudinal direction

Further investigations were performed on the vertical elements in terms of the shear walls, with the main structural element resisting the applied lateral load. Table 1 presents the peak base overturning moments and compares the shear and axial forces computed for different shear walls distributed in the transverse direction of the twenty-five-story building under the NS components of the Niigata earthquake motions with and without sequences along with listing the values of the computed straining actions of the selected shear walls under dynamic RS analysis. As can be observed in Table 1, the high-rise building under the regular Niigata records demonstrated a considerable reduction in the obtained peak straining action responses compared with those obtained under the sequential Niigata records. These captured peak responses clearly indicate that the straining actions attracted by the lateral-force-resisting system increased owing to the existence of sequences. The induced peak responses obtained via the dynamic RS analysis showed good agreement with the values for the shear walls as calculated under the Niigata records without sequences. However, a significant difference can be observed with the values obtained under the Niigata records with sequences. From a structural design perspective, the designed steel reinforcements and concrete sections of the shear walls may be insufficient for withstanding the induced straining actions due to the applied seismic actions incorporating sequences, which may cause severe damage to some of the designed shear walls. In structural design applications, sufficient attention should be paid to adequately reflecting the higher uncertainty in ground motions with sequences compared with normal horizontal ground motion earthquakes.

5.6. Global damage index

Owing to their significant role in determining the damage index using Cosenza and Fajfar's damage model, both inelastic deformation and dissipated energy responses were used as measures to assess the induced damage of the high-rise building in both the longitudinal and transverse directions. The global damage indices vs. time are displayed in Figure 15 for the directions of analysis under the scaled Niigata earthquake records with and without sequences. Figure 15 shows the variation of the obtained damage index in relation to time until the maximum index value is reached for the two directions under the ground excitations of interest. Here, it can be inferred that the use of the Niigata earthquake records without pulses led to minor and negligible damage to the building in the transverse and longitudinal directions. In contrast, as Figure 15 shows, the existence of sequences either in the NS or the EW components of the excitations typically

Table 1. Maximum inelastic response quantities for shear walls and cores under Niigata ground motion inputs in the NS direction

Pier label	NIG028-NS			CHUETSU-NIG028-NS			Design results (RS)		
	P (kN)	*V* (kN)	*M* (kN.m)	*P* (kN)	*V* (kN)	*M* (kN.m)	*P* (kN)	*V* (kN)	*M* (kN.m)
SW1	291	245	1734	455	439	2738	401	278	1927
SW2	903	212	1542	1605	429	2497	1262	201	1714
SW3	853	190	2002	1637	412	3095	1150	132	2225
SW5	409	135	1066	912	243	1649	608	90	1185
SW7	403	148	1260	1053	227	1930	652	103	1400
SW9	987	153	1464	2018	227	2320	1455	117	1627
SW11	389	252	1872	707	442	3270	537	230	2081
SW13	540	545	7963	1594	1092	13279	1040	599	8848
SW19	744	798	11173	1582	1504	16795	1050	896	12415

Note: P – peak axial compression load; *V* – peak shear force; *M* – peak overturning moment at base.

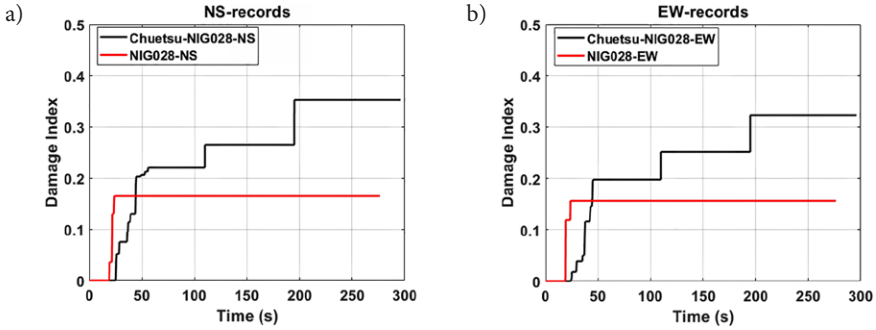

Figure 15. Damage index time-histories obtained under the NS and EW components of the Niigata records with and without sequences in the: a – transverse direction and b – longitudinal direction

increased the Cosenza and Fajfar damage index values of the developed model. The maximum damage values were reported and the calculated percentage of increase in damage index values based on the reported peak values indicated a significant contribution of the sequences in magnifying the damage to the buildings. The status of the structure during simulation under the different records of the Niigata earthquake in both directions as well as the evolution of the damage index in both directions were numerically reported. The captured peak damage index values were close to 0.18 and 0.17 under the Niigata records without sequences for the NS and EW directions, respectively. However, when using the Niigata records with sequences for the excitation in the NS and EW directions, the peak damage index values were around 0.37 and 0.33, respectively. As these values were significantly different, the existence of sequences maximizes the damage values and consequently magnifies the probability of damage to the structures. As is notable from the plotted results shown in Figure 15, both directions experienced a sudden increment in the damage level as well as a variation in the damage value for the building model excited under records containing sequences. Moreover, both from the figure and from the two principal directions of consideration, the plots of damage index vs. time under the Niigata records with sequences exhibited certain intermediate steps before reaching the peak damage index value. However, the plots under the Niigata records without sequences went from zero to the maximum value in very few steps compared with those presented under the records with sequences. From the structural design, damage, and practical perspectives, the latter aspect is clearly the most hazardous and risky.

Owing to the existence of sequences that cause an accumulation of inelastic deformations, the structure achieved damage index values that can be deemed relatively high, regardless of the direction of the application of the records. Consequently, the structure should be evacuated for performing maintenance and repairs. Further, the captured damage index value was sufficiently removed from the assigned value for collapse (0.80). However, the possibility of damage to high-rise buildings with the occurrence of earthquakes with multiple peaks still needs to be appropriately considered.

Conclusions

Linear and nonlinear dynamic analysis were used to analyze a typical high-rise RC shear-wall building located in Dubai following the requirements of the ASCE 7-16 standard (ASCE, 2017). Single and multiple records of the Niigata earthquake were applied to the transverse and

longitudinal directions of the considered herein building. The analysis results for the considered typical high-rise RC building indicate that:

- The overall seismic performance for the typical RC building considered herein under the design-level of a single earthquake is acceptable compared with those obtained via the dynamic RS analysis.
- There is a risk of failure of the typical building owing to an underestimation of seismic demands at the design stage in relation to the induced seismic demand under a multi-shock earthquake scaled to fit the seismic zone intensity of the building's location.
- The results indicated that a multi-shock earthquake may significantly influence the increment in displacement, acceleration, shear, and moment demands, which will exceed the captured design values, regardless of the direction of excitation.
- A multi-shock earthquake will also result in a larger damage index for the typical high-rise building compared with a single-shock earthquake.
- The current design codes may be inadequate for preventing failure in similar high-rise buildings to the studied one under a multi-shock earthquake.
- Strong consideration should be given to adequately reflect the higher uncertainty in repeated ground-motion sequences compared with that in single ground motion events within the design codes.

Acknowledgements

We thank IAU to give us the opportunity for this research work.

Funding

The authors received no specific funding for this study.

Conflicts of interest

The authors declare that they have no conflicts of interest to report regarding the present study.

References

Abdelnaby, A. E. (2012). *Multiple earthquake effects on degrading reinforced concrete structures* [PhD dissertation]. University of Illinois at Urbana-Champaign, Illinois.

Amadio, C., Fragiacomo, M., & Rajgelj, S. (2003). The effects of repeated earthquake ground motions on the non-linear response of SDOF systems. *Earthquake Engineering & Structural Dynamics*, *32*(2), 291–308. https://doi.org/10.1002/eqe.225

American Society of Civil Engineers. (2017). *Minimum design loads and associated criteria for buildings and other structures* (Standard No. ASCE 7-16).

Bao, X., Zhang, D., & Zhai, C. H. (2019). Fragility analysis of a containment structure under far-fault and near-fault seismic sequences considering post-mainshock damage states. *Engineering Structures*, *198*, 239–287. https://doi.org/10.1016/j.engstruct.2019.109511

Chandramohan R., Baker, J. W, & Deierlein, G. G. (2016). Quantifying the influence of ground motion duration on structural collapse capacity using spectrally equivalent records. *Earthquake Spectra*, *32*(2), 927–950. https://doi.org/10.1193/122813eqs298mr2

Chase, R. E., Liel, A. B., Luco, N., & Baird, B. W. (2019). Seismic loss and damage in light-frame wood buildings from sequences of induced earthquakes. *Earthquake Engineering & Structural Dynamics*, *489*(12), 1365–1383. https://doi.org/10.1002/eqe.3189

Cosenza, C., Manfredi, M., & Ramasco, R. (1993). The use of damage functionals in earthquake engineering: A comparison between different methods. *Earthquake Engineering & Structural Dynamics*, *22*(10), 855–868. https://doi.org/10.1002/eqe.4290221003

Di Sarno, L. (2013). Effects of multiple earthquakes on inelastic structural response. *Engineering Structures*, *56*, 673–681. https://doi.org/10.1016/j.engstruct.2013.05.041

Elnashai, A. S., Bommer, J. J., & Martinez-Pereira, A. (1998). Engineering implications of strong motion records from recent earthquakes. In *Proceedings of 11th European Conference on Earthquake Engineering* (pp. 6–11), Paris, France.

Fajfar, P. (1992). Equivalent ductility factors, taking into account low-cyclic fatigue. *Earthquake Engineering & Structural Dynamics*, *21*(10), 837–848. https://doi.org/10.1002/eqe.4290211001

Faisal, A., Majid, T. A., & Hatzigeorgiou, G. D. (2018). Investigation of story ductility demands of inelastic concrete frames subjected to repeated earthquakes. *Soil Dynamics and Earthquake Engineering*, *44*, 42–53. https://doi.org/10.1016/j.soildyn.2012.08.012

Goda, K., & Taylor, C. A. (2012). Effects of aftershocks on peak ductility demand due to strong ground motion records from shallow crustal earthquakes. *Earthquake Engineering & Structural Dynamics*, *41*(15), 2311–2330. https://doi.org/10.1002/eqe.2188

Goda, K., & Salami, M. R. (2014). Inelastic seismic demand estimation of wood-frame houses subjected to mainshock-aftershock sequences. *Bulletin of Earthquake Engineering*, *12*, 855–874. https://doi.org/10.1007/s10518-013-9534-4

Ghosh, J., Padgett, E., & Sánchez-Silva, M. (2015). Seismic damage accumulation in highway bridges in earthquake-prone regions. *Earthquake Spectra*, *31*(1), 115–135. https://doi.org/10.1193/120812EQS347M

Hameed, A., Saleem, M., Qazi, A.U., Saeed, S., Ilyas, M., & Bashir, A. (2012). Mitigation of seismic pounding between adjacent buildings. *Pakistan Journal of Science*, *64*(4), 326–333.

Hatzigeorgiou, G. D., & Beskos, D. E. (2009). Inelastic displacement ratios for SDOF structures subjected to repeated earthquakes. *Engineering Structures*, *31*(11), 2744–2755. https://doi.org/10.1016/j.engstruct.2009.07.002

Hatzigeorgiou, G. D. (2010). Ductility demand spectra for multiple near- and far-fault earthquakes. *Soil Dynamics and Earthquake Engineering*, *30*(4), 170–183. https://doi.org/10.1016/j.soildyn.2009.10.003

Hatzivassiliou, M., & Hatzigeorgiou, G. D. (2015). Seismic sequence effects on three-dimensional reinforced concrete buildings. *Soil Dynamics and Earthquake Engineering*, *72*, 77–88. https://doi.org/10.1016/j.soildyn.2015.02.005

Jalayer, F., & Ebrahimian, H. (2017). Seismic risk assessment considering cumulative damage due to aftershocks. *Earthquake Engineering & Structural Dynamics*, *46*(3), 369–389. https://doi.org/10.1002/eqe.2792

Kunnath, S. K., Reinhorn, A. M., & Park, Y. J. (1990). Analytical modeling of inelastic seismic response of RC structures. *Journal of Structural Engineering*, *116*(4), 996–1017. https://doi.org/10.1061/(ASCE)0733-9445(1990)116:4(996)

Li, Y., Song, R., & Van De Lindt, J. W. (2014). Collapse fragility of steel structures subjected to earthquake mainshock-aftershock sequences. *Journal of Structural Engineering*, *140*(12), 621–634. https://doi.org/10.1061/(ASCE)ST.1943-541X.0001019

Luco, N., Bazzurro, P., & Cornell, C. A. (2004). Dynamic versus static computation of the residual capacity of mainshock-damaged building to withstand an aftershock. In *Proceedings of the 13th World Conference on Earthquake Engineering* (Paper No. 2405, pp. 6–11), Vancouver, Canada.

McCabe, S. L., & Hall, W. J. (1989). Assessment of seismic structural damage. *Journal of Structural Engineering*, *115*(9), 2166–2183. https://doi.org/10.1061/(ASCE)0733-9445(1989)115:9(2166)

Mwafy, A., Elnashai, A. S., Sigbjörnsson, R., & Salama, A. (2006) Significance of severe distant and moderate close earthquakes on design and behavior of tall buildings. *Structural Design of Tall and Special Buildings*, *15*(4), 391–416. https://doi.org/10.1002/tal.300

Parisi, F., & Augenti, N. (2013). Earthquake damages to cultural heritage constructions and simplified assessment of artworks. *Engineering Failure Analysis*, *34*, 735–760. https://doi.org/10.1016/j.engfailanal.2013.01.005

Parekar, S. D., & Datta, D. (2020). Seismic behaviour of stiffness irregular steel frames under mainshock–aftershock. *Asian Journal Civil Engineering*, *21*, 857–870. https://doi.org/10.1007/s42107-020-00245-z

Park, Y. J., & Ang, A. H. (1985). Mechanistic seismic damage model for reinforced concrete. *Journal of Structural Engineering*, *111*(4), 722–739. https://doi.org/10.1061/(ASCE)0733-9445(1985)111:4(722)

Pomonis, A., Saito, K., Chian, S. C., Fraser, S., Goda, K., & Macabuag, J. (2011). *The Mw 9.0 Tohoku earthquake and tsunami of 11 March 2011*. Earthquake Engineering Field Investigation Team (EEFIT), The Institution of Structural Engineers, London, UK.

Powell, G. H., & Allahabadi, R. (1988). Seismic damage prediction by deterministic methods: concepts and procedures. *Earthquake Engineering & Structural Dynamics*, *16*, 719–734. https://doi.org/10.1002/eqe.4290160507

Penna, A., Morandi, P., Rota, M., Manzini, C. F., Porto, F., & Magenes, G. (2014). Performance of masonry buildings during the Emilia 2012 earthquake. *Bulletin of Earthquake Engineering*, *12*(5), 2255–2273. https://doi.org/10.1007/s10518-013-9496-6

Ruiz-García, J., & Negrete-Manriquez, J. (2011). Evaluation of drift demands in existing steel frames under as-recorded far-field and near-fault mainshock–aftershock seismic sequences. *Engineering Structures*, *33*, 621–634. https://doi.org/10.1016/j.engstruct.2010.11.021

Ruiz-Garcíaa, J., Yaghmaei-Sabegh, B., & Bojórquezc, S. E. (2018). Three-dimensional response of steel moment-resisting buildings under seismic sequences. *Engineering Structures*, *175*(15), 399–414. https://doi.org/10.1016/j.engstruct.2018.08.050

Saleem, M., & Tsubaki, T. (2010). Multi-layer model for pull-out behavior of post-installed anchor. *Proceedings FRAMCOS-7*, *Fracture Mechanics of Concrete Structures*, *2*, 823–830.

Saleem, M., & Nasir, M. (2016). Bond evaluation of concrete bolts subjected to impact loading. *Materials and Structures*, *49*, 3635–3646. https://doi.org/10.1617/s11527-015-0745-9

Scawthorn, C., & Rathje, E. M. (2006). The 2004 Niigata Ken Chuetsu, Japan. *Earthquake Spectra*, *22*(1), 1–8. https://doi.org/10.1193/1.2172259

Soureshjani, O., & Massumi, A. (2022). Seismic behavior of RC moment resisting structures with concrete shear wall under mainshock–aftershock seismic sequences. *Bulletin of Earthquake Engineering*, *20*, 1087–1114. https://doi.org/10.1007/s10518-021-01291-x

Wen, W., Ji, D., Zhai, C., Li, X., & Sun, P. (2018). Damage spectra of the mainshock-aftershock ground motions at soft soil sites. *Soil Dynamics and Earthquake Engineering*, *115*, 815–825. https://doi.org/10.1016/j.soildyn.2018.08.016

Williams, M. S., & Sexsmith, R. G. (1995). Seismic damage indices for concrete structures: a state-of-the-art review. *Earthquake Spectra*, *11*(2), 319–349. https://doi.org/10.1193/1.1585817

Yaghmaei-Sabegh, S., & Ruiz-García, J. (2016). Nonlinear response analysis of SDOF systems subjected to doublet earthquake ground motions: A case study on 2012 Varzaghan–Ahar events. *Engineering Structures*, *110*, 281–292. https://doi.org/10.1016/j.engstruct.2015.11.044

Zimmaro, P., Scasserra, G., & Stewart, G. P. (2018). Strong ground motion characteristics from 2016 Central Italy earthquake sequence. *Earthquake Spectra*, *34*(4), 1611–1637. https://doi.org/10.1193/091817EQS184M

Zhai, C., Ji, D., Wen, W., Lei, W., Xie, L., & Gong, M. (2016). The inelastic input energy spectra for main shock–aftershock sequences. *Earthquake Spectra*, *32*(4), 2149–2166. https://doi.org/10.1193/121315EQS182M